


RESEARCH ARTICLE

Theta band power increases in the posterior hippocampus predict successful episodic memory encoding in humans

Jui-Jui Lin¹ | Michael D. Rugg² | Sandhitsu Das³ | Joel Stein³ |
Daniel S. Rizzuto⁴ | Michael J. Kahana⁴ | Bradley C. Lega¹ 

¹Department of Neurological Surgery, University of Texas, Southwestern Medical Center, Dallas, Texas 75390

²Center for Vital Longevity, University of Texas at Dallas, Dallas, Texas 75390

³Department of Radiology, University of Pennsylvania, Philadelphia, Pennsylvania 19104

⁴Department of Psychology, University of Pennsylvania, Philadelphia, Pennsylvania 19104

Correspondence

B. Lega, UT-Southwestern, Neurological Surgery MS 8855, 5323 Harry Hines Blvd, Dallas 75390, TX.
Email: bradlega@gmail.com

Funding information

Funding in part via UT Brain Seed Grant #366582, NIH R21 NS095094 and DARPA Restoring Active Memory project; DARPA Restoring Active Memory (RAM) program (Cooperative Agreement N66001-14-2-4032)

Abstract

Functional differences in the anterior and posterior hippocampus during episodic memory processing have not been examined in human electrophysiological data. This is in spite of strong evidence for such differences in rodent data, including greater place cell specificity in the dorsal hippocampus, greater sensitivity to the aversive or motivational content of memories in ventral regions, connectivity analyses identifying preferential ventral hippocampal connections with the amygdala, and gene expression analyses identifying a dorsal–ventral gradient. We asked if memory-related oscillatory patterns observed in human hippocampal recordings, including the gamma band and slow-theta (2.5–5 Hz) subsequent memory effects, would exhibit differences along the longitudinal axis and between hemispheres. We took advantage of a new dataset of stereo electroencephalography patients with simultaneous, robotically targeted anterior, and posterior hippocampal electrodes to directly compare oscillatory subsequent memory effects during item encoding. This same data set allowed us to examine left–right connectivity and hemispheric differences in hippocampal oscillatory patterns. Our data suggest that a power *increase* during successful item encoding in the 2.5–5 Hz slow-theta frequency range preferentially occurs in the posterior hippocampus during the first 1,000 ms after item presentation, while a gamma band power increase is stronger in the dominant hemisphere. This dominant–nondominant pattern in the gamma range appears to reverse during item retrieval, however. Intrahippocampal phase coherence was found to be stronger during successful item encoding. Our phase coherence data are also consistent with existing reports of a traveling wave for theta oscillations propagating along the septotemporal (longitudinal) axis of the human hippocampus. We examine how our findings fit with theories of functional specialization along the hippocampal axis.

KEYWORDS

theta, episodic memory, anterior hippocampus, posterior hippocampus, subsequent memory effect

1 | INTRODUCTION

Rodent hippocampal theta oscillations have demonstrated a reliable relationship to memory encoding in investigations involving multiple memory modalities and behavioral tasks, but in humans the data have been mixed. There is strong evidence of a gamma band power increase during successful encoding (a positive subsequent memory effect, SME), but a commensurate theta-range positive effect has not been consistently observed in human hippocampal electrodes (Burke et al., 2014; Jacobs, 2014; Sederberg et al., 2007; Watrous, Fried, & Ekstrom,

2011). However, there is evidence that a subset of hippocampal contacts exhibit significant positive effects in the 2–5 Hz frequency range, that is, at the lower edge of the traditional 3–8 Hz theta band (Lega, Jacobs, & Kahana, 2011; Watrous et al., 2011). Previous studies, using hippocampal depth electrodes inserted principally via open craniotomy, have focused on the anterior portion of the hippocampus, with relatively few contacts in the posterior body and tail. There is considerable evidence in the rodent literature for functional and structural differences between the dorsal (posterior in humans) and ventral (anterior in humans) portions of the hippocampus (Moser & Moser, 1998; Fanselow

& Dong, 2010; Poppenk, Evensmoen, Moscovitch, & Nadel, 2013; Strange, Witter, Lein, & Moser, 2014). Differences in spatial processing (dorsal), contextual memory (dorsal), and emotional/aversive/motivational content of memories (ventral) have been observed along the septotemporal axis (analogous to the anterior–posterior longitudinal axis in humans) (Henke, 1990; Fanselow & Dong, 2010; Maggio & Segal, 2009; Matus-Amat, Higgins, Barrientos, & Rudy, 2004; Moser, Moser, & Andersen, 1993). There has been equivocal support for longitudinal specialization in human hippocampal function, with studies that report an anterior–posterior transition of activation for encoding versus retrieval (Greicius et al., 2003) and for spatial versus nonspatial processing (Ryan, Lin, Ketcham, & Nadel, 2010), although conflicting data across memory tasks have spawned more nuanced theories of longitudinal specialization positing differences in the “scale” of information processing (Poppenk et al., 2013). However, there have as yet been no direct brain recordings in humans to provide evidence in support of these views or to directly link human data with results in animals. Most human hippocampal data has been collected from the anterior hippocampus, which shows consistent gamma band power elevations during successful encoding of episodic memories and during spatial navigation (Ekstrom, Nanthia, David, Itzhak, & Susan, 2009; Sederberg et al., 2007). There is also evidence of a strong low-frequency power *decrease* most evident in the 5–9 Hz frequency band (a negative SME) for these recordings (Ekstrom et al., 2005).

Hemispheric differences in hippocampal activation during mnemonic processing have been observed most strongly in spatial navigation, which is associated with stronger activation effects in the nondominant hemisphere in noninvasive (Abrahams, Pickering, Polkey, & Morris, 1997; Bohbot et al., 1998; Pu, Cornwell, Cheyne, & Johnson, 2017) and invasive studies in humans (Jacobs et al., 2010). Strong lateralization for episodic memory has been less consistently observed in fMRI (Fletcher, Frith, & Rugg, 1997), although structural data (Ezzati et al., 2016) suggest verbal memory stimuli are encoded more strongly in the left hemisphere. Human electrophysiological data examining interhemispheric connectivity have been rare due to the implantation arrays in traditional datasets.

Stereo electroencephalography has gained increasing popularity as a complement to grid electrode studies for intracranial seizure monitoring because it is less invasive and it offers the ability to sample from multiple subcortical structures in both hemispheres (Gonzalez-Martinez et al., 2013). With robotic assistance, the accuracy of electrode placement is submillimeter and this permits the use of laterally-inserted depth electrodes into the anterior and posterior hippocampus, with dorsal hippocampal contacts located posterior to where the hippocampus begins to curve medially around the thalamus. Existing iEEG datasets that have been collected as subjects performed episodic memory tasks, with electrodes placed via open craniotomy, have almost exclusively included laterally-inserted anterior hippocampal electrode contacts (Lega et al., 2011; Watrous et al., 2011).

We took advantage of a unique dataset of 23 participants implanted with both anterior and posterior laterally inserted hippocampal depth electrodes to examine oscillatory differences between the

anterior and posterior human hippocampus. All of these patients had electrodes in both locations simultaneously, permitting us to examine phase relationships for the oscillations that exhibited mnemonically-relevant properties. 12 of these patients had bilaterally inserted (anterior) hippocampal electrodes, permitting us also to examine left–right connectivity during memory encoding, revealing left–right synchrony that predicts successful item encoding 600–1,000 ms after the onset of item presentation. We provide evidence that the slow-theta power increase previously reported in a minority of hippocampal recordings (Lega et al., 2011; Watrous et al., 2011) is strongest in the posterior hippocampus (in both hemispheres), while the gamma band subsequent memory effect does not differ along the longitudinal axis but is stronger in the language dominant hemisphere during encoding but not item retrieval. We place our findings into the context of existing animal and human electrophysiological and imaging data and examine our results as they pertain to novel theories of human hippocampal processing.

2 | MATERIALS AND METHODS

2.1 | Participants

23 subjects with medication-resistant epilepsy who underwent stereo-electroencephalography surgery with the goal of identifying their ictal onset region(s) participated in the study during their monitoring period. Participants came from the UT Southwestern epilepsy surgery program over a period of two years. All participants with at least one anterior–posterior hippocampal electrode pair that was not the site of seizure onset were included in the study. Subjects had up to 15 intracranial depth electrode implants at locations specified by the neurology team, two of which included targeting the anterior and posterior segment of the hippocampus using a lateral approach with robotic assistance for submillimeter accuracy. Each electrode contained ten contacts spaced 3–5 mm apart. Final electrode localization determination as in or out of the hippocampus was made by expert neuroradiology review of the electrode contact locations. In planning, demarcation along the hippocampal axis was made using the junction of the tectum and tegmentum in the coronal plane; this is slightly posterior to segmental demarcation at the uncus apex described in Poppenk et al. (2013). Figure 1 shows MRI localization of hippocampal electrodes and contacts for one subject. Overall, there were 71 anterior and 70 posterior hippocampal electrodes included in the dataset. These were also broken down as 65 right sided and 76 left sided electrodes, though only 31 of these electrodes were from the 12 patients with bilateral contacts. Hemisphere of language dominance was determined by preoperative Wada or fMRI testing prior to implantation, as part of routine clinical practice.

2.2 | Behavioral task

The participants performed a verbal free recall task, in which visually presented words from a predetermined pool of common nouns were presented on a laptop monitor one at a time for 1.6 s each followed by a blank screen of 4 s with 100 ms of random jitter for a total of 15 memory items in a single list. Each list was followed by a 30 s period of simple

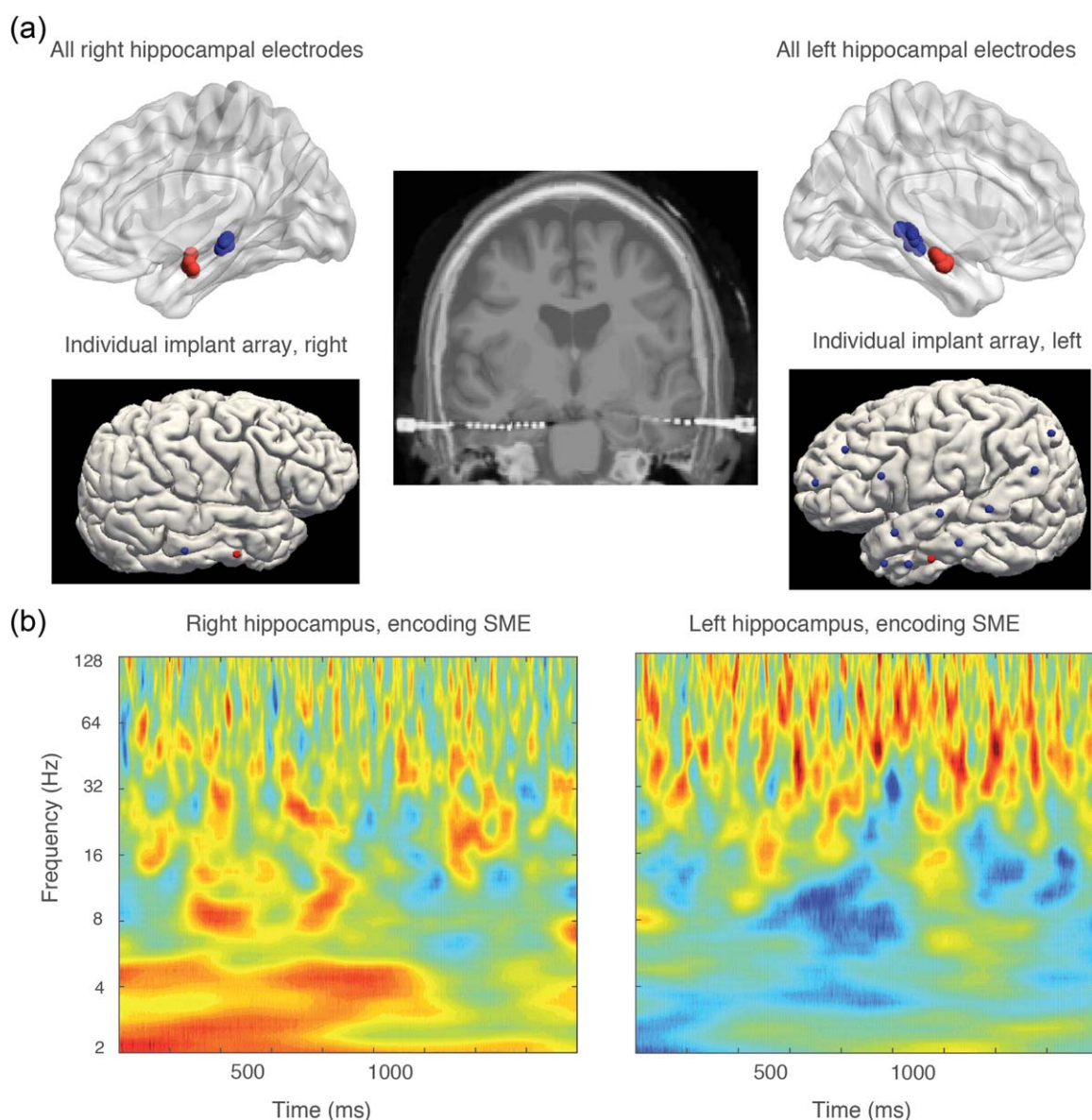


FIGURE 1 Example of power subsequent memory effect in left and right sided contacts. (a) (top row) shows location of left and right hippocampal contacts across all subjects in the dataset using normalized electrode coordinates. Panels beneath are from a single patient showing electrode locations from a stereo EEG evaluation for a patient contributing anterior and posterior hippocampal data on a surface rendering (electrode entry locations); middle image shows these electrodes in coronal cross section. (b) shows the subsequent memory effect in the right and left hippocampus, respectively from the same patient whose electrodes are shown in (a). Gamma subsequent memory effect is stronger in the left sided contact for this patient, a pattern that persists across subjects. The right-sided SME also is stronger in the slow-theta range for this subject [Color figure can be viewed at wileyonlinelibrary.com]

math distractors in the form of $A + B + C = ??$ to limit rehearsal. Participants were instructed to recall as many words as possible from the list just presented to them in no particular order within a 30 s recall period (memory retrieval). This was done 25 times per session and each participant completed from one to three sessions. Further details of the task are described in Sederberg, Kahana, Howard, Donner, and Madsen (2003).

2.3 | Subsequent memory effect analysis

We sought to compare oscillatory power from successfully encoded memory items to that of unsuccessfully encoded items to identify a

relationship between differences in oscillatory power and likelihood of subsequent recall. Signal was sampled at 1 kHz on a Nihon-Koden platform. Line noise was notch filtered, and we excluded activity from electrodes that were the site of seizure onset locations or frequent interictal activity (total of 5 electrodes from two patients). Power analyses were conducted using a Laplacian reference scheme for consistency with other studies and to take advantage of favorable signal-to-noise characteristics (Lega, Jacobs, & Kahana, 2011; Sederberg et al., 2007; Zhang & Jacobs, 2015). For connectivity/phase coherence analysis we used a bipolar rereference for hippocampal signal in which hippocampal contacts were referenced to adjacent white matter. We used

a kurtosis algorithm (with threshold of 4) to exclude abnormal events and interictal activity. The power values were extracted from 1800 ms time windows following the appearance of the study item using Morlet wavelets with width of six at 49 log-spaced frequencies centered at $2^{(n/8)}$, $n = 8$: 64 (Tallon-Baudry, Olivier, Claude, & Jacques, 1997). Power values across the time series derived from recalled events were then as compared to values from nonrecalled events via a Wilcoxon rank-sum test at each time-frequency point. Within the rank-sum test, we incorporated a permutation procedure (1000 iterations) to generate an unbiased estimate of the type 1 error rate (Sederberg et al., 2003). We generated a p value by identifying the position of the true ranksum statistic from the test applied to real data with 1000 ranksum values generated from shuffling recalled and nonrecalled event labels. We then applied normal inverse transformation to the p values matrices of each electrode to convert them to Z values to combine across electrodes and subjects.

Our *a priori* hypotheses were that we would observe a difference between anterior and posterior hippocampal activity and left versus right hippocampal activity in gamma and slow-theta activity; we therefore statistically compared the SME for different hippocampal locations using a t -test applied to the distribution of Z values from each time-frequency step for electrodes within each hippocampal region. To correct for multiple comparisons across these six frequency bands, we used a Bonferroni's correction after averaging power within each band. We also applied a clustering requirement by which we required that significant effects persisted for at least one continuous half cycle of a given oscillation. Reported significant results for these power analyses are from a random effects model, in which power values were averaged for all electrodes within each subject before comparing distributions of language dominant/non dominant or ventral/dorsal contacts. In general, we used nonparametric statistical tests when comparing distributions of oscillatory power and parametric tests when comparing distributions of test statistics (Z values).

2.4 | Phase analysis

The oscillatory phase for each time-frequency pixel was extracted using the same method as described for power using Morlet wavelets. The resulting phase values were used to determine oscillatory synchrony between anterior hippocampal contacts and posterior hippocampal contacts. Calculation of synchrony was implemented with Rayleigh tests including a shuffle procedure for randomization (bootstrapping), generating a phase locking statistic (PLS) as described previously (Lachaux, Rodriguez, Martinerie, & Varela, 1999). A separate distribution of PLS values for recalled and nonrecalled events was obtained for all dorsal-ventral and dominant-nondominant hippocampal pairs for each subject (total of 137 left-right pairs, 222 dorsal-ventral pairs). A subsequent memory effect in dominant-nondominant hippocampal synchrony was analyzed by running a t -test between distributions Z values of recalled events and of nonrecalled events for all contact pairs from all subjects. This resulted in a p value at every time-frequency step. Within the time windows that revealed significant phase coherence, we calculated the mean phase difference for each

electrode pair across trials. Phase reset analysis was performed by testing the uniformity of the distribution of phase values across trials at each time step *within* a given electrode, then comparing the distributions of Z values from recalled and nonrecalled trials across electrodes (Rizzuto, Madsen, Bromfield, Schulze-Bonhage, & Kahana, 2006). We calculated the speed of propagation for a presumed traveling wave centered at 4 Hz in the hippocampus (Zhang & Jacobs, 2015) by calculating the mean phase difference (for time points exhibiting significant phase coherence, $p < 0.05$) between anterior and posterior hippocampal contacts. Using the Euclidean distance between the two electrode locations calculated via Talairach coordinates for the electrodes, the frequency of the oscillation, and this phase offset, we were able to calculate the speed of propagation.

2.5 | Analysis during item retrieval period

To analyze brain oscillatory activity during retrieval, one must create a comparison condition for the period immediately prior to item retrieval during which the representation of a memory item is being reinstated. Because false recall events were rare, we employed a previously published method (Burke et al., 2014) by which retrieval events were filtered to ensure there were not any other retrieval events within 1500 ms before or 500 ms afterward in the time series, and then statistically comparing a distribution of these 1400 ms epochs to a control distribution of 1 s time segments drawn from within the retrieval epoch. The results we present are from correct retrieval events only.

3 | RESULTS

3.1 | Anterior-posterior differences in subsequent memory effects

We analyzed 23 subjects with stereo EEG electrodes inserted into the anterior and posterior hippocampus. The average distance between anterior and posterior electrodes was 22.4 mm (range 18–31 mm). We quantified the subsequent memory effect for the 71 anterior and 70 posterior electrodes using a ranksum test with shuffle procedure; the aggregate SME from each subregion (average Z value from this shuffle test) is shown in Figure 2, top panel. We directly compared the SME for anterior and posterior electrodes at the subject level by averaging Z values for all electrodes in each subject and then comparing the resulting distributions using a t -test. Results of this anterior-posterior comparison in time-frequency space are shown in the lower left panel in Figure 2 (filtered for $p < .05$ for one continuous half cycle of the oscillation); they suggest there is a positive SME in the 2.5–5 Hz slow-theta range that is significantly greater in the posterior than anterior hippocampus. We further tested this observation by averaging the Z values within each frequency band before performing the t -test between regions (Figure 2, lower right plot) and then Bonferroni's correcting the resultant p values ($t(22) > 2.9$ significance threshold for corrected values, paired t -test). The slow-theta positive SME is significantly greater for a continuous half cycle for the posterior hippocampus centered at 500 ms after presentation of the memory items. In the anterior

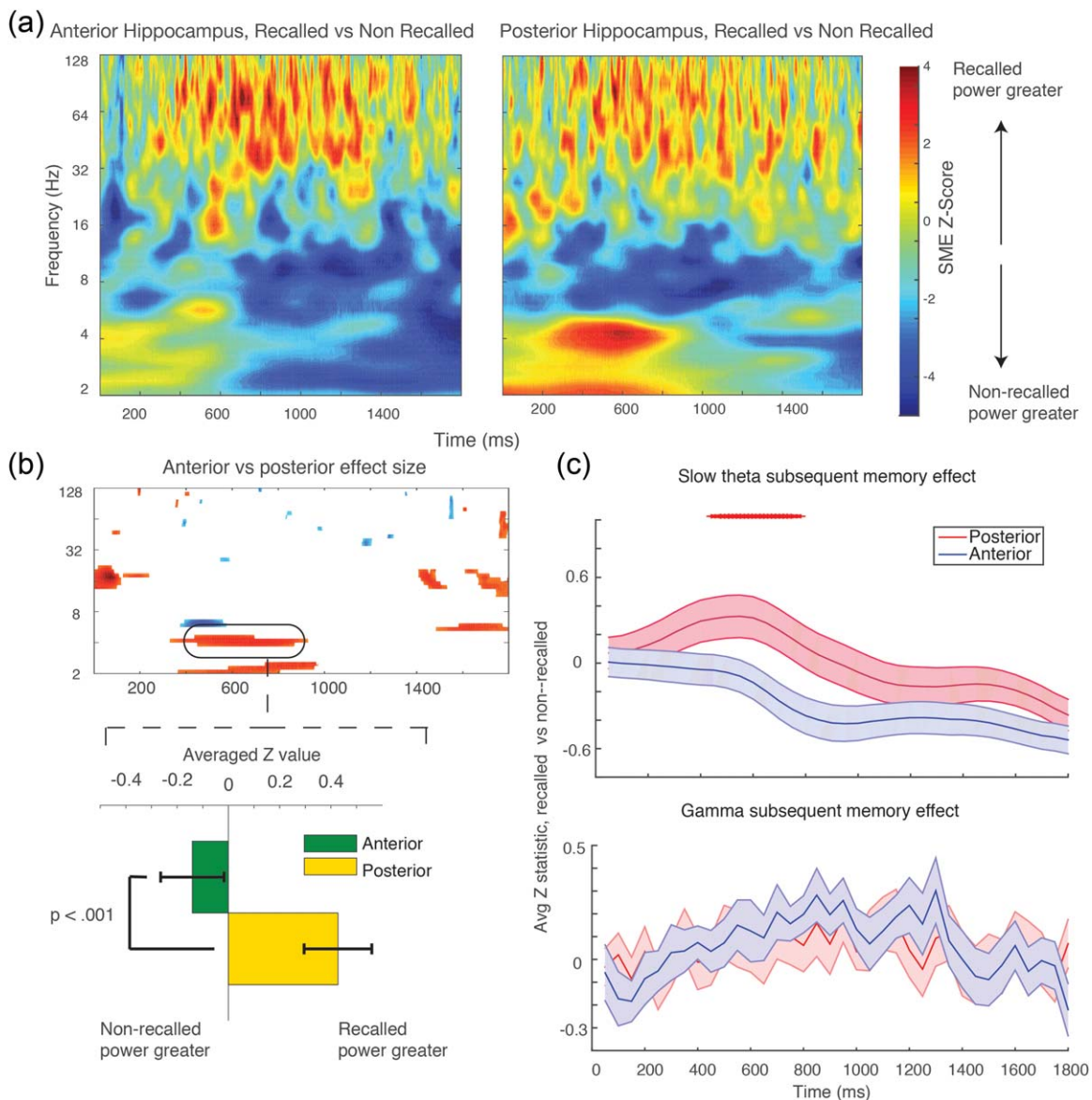


FIGURE 2 SME in anterior versus posterior hippocampus. (a) Shows aggregate subsequent memory effect *across all electrodes* (effect size) in anterior (left panel) and posterior (right panel) time–frequency plots. (b) Shows time–frequency plot shows pixels across all subjects (averaging signal from all electrodes in each subject's hippocampus) that survive correction ($p < .05$ for one continuous half cycle of the oscillation, t -test across 23 subjects SME Z values). Red colors indicate posterior > anterior effect size; blue is anterior > posterior. Bar plot below show the mean slow-theta SME for anterior and posterior contacts for the highlighted time–frequency segment (SME Z values averaged in time–frequency window highlighted, t -test across 23 subjects). This plot shows that the observed SME difference is driven by a slightly negative effect in the anterior hippocampus versus a positive effect in the posterior hippocampus in the first 1,000 ms after item presentation. (c) Upper plot shows the average effect in the slow-theta band across the time series. Red tick marks indicate time points at which SME difference survives Bonferroni's correction ($p < .008$) for one continuous half cycle. There are no significant differences in the gamma band shown in the lower panel [Color figure can be viewed at wileyonlinelibrary.com]

hippocampus, there is a negative subsequent memory effect that is strongest in the second half of the time series, though the comparison with the posterior hippocampus does not survive correction at the subject level (corrected $p > .05$). These data suggest that sampling from the anterior hippocampus exclusively will underestimate a positive slow-theta effect during item encoding, and that there may be human analogues of functional differences observed along the dorsal–ventral axis in rodent hippocampi. The gamma band subsequent memory

effect is not significantly different between anterior and posterior contacts, however (see Figure 2, lower right).

We further studied the properties of this slow-theta oscillation by examining anterior–posterior connectivity during successful encoding. We quantified connectivity using the phase locking statistic (PLS) between anterior and posterior contacts, taking advantage of the unique properties of our stereo EEG dataset to capture information from both locations simultaneously with good confidence about the

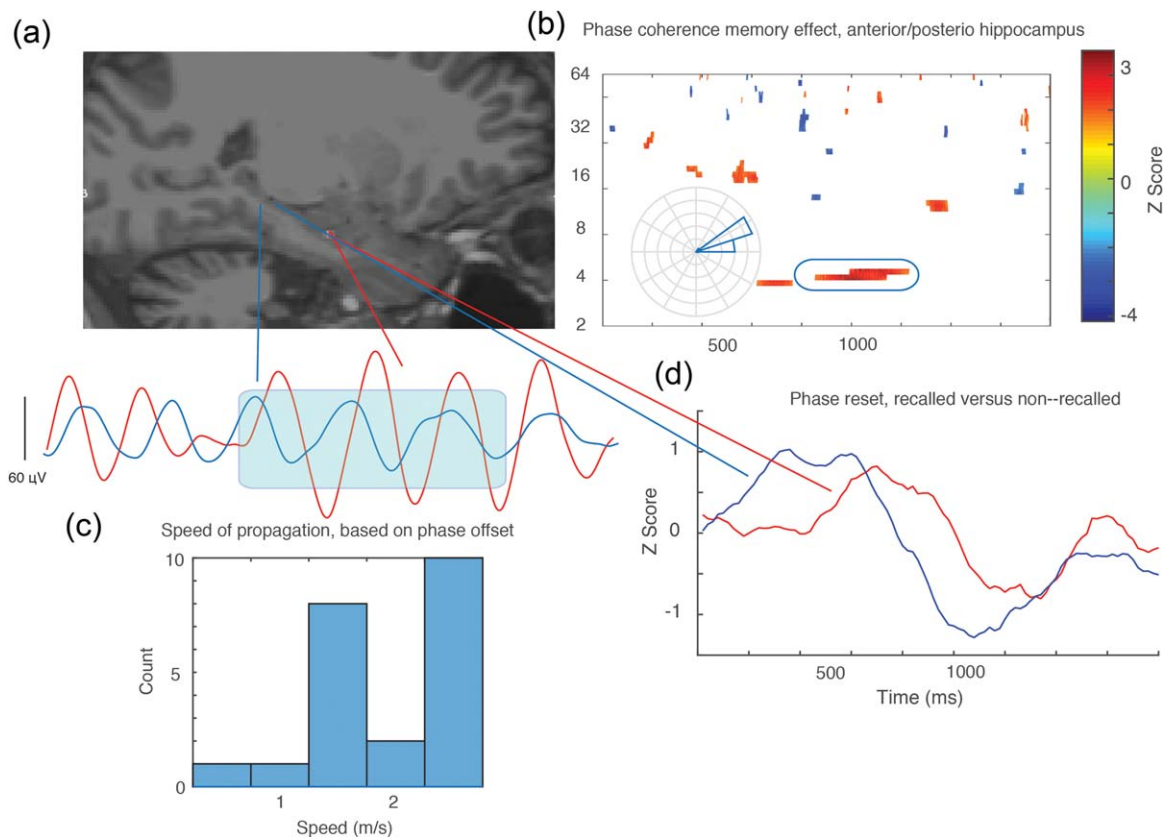


FIGURE 3 Phase coherence along dorsal–ventral hippocampal axis during item encoding. (a) Electrode locations in dorsal and ventral hippocampus in an experimental subject with single trial slow-theta wave from this same patient plotted below (1800 ms time window). (b) Significant connectivity subsequent memory effect (*t*-test across 23 subjects, comparing connectivity in recalled versus nonrecalled events), with time–frequency points with $p < .05$ for one continuous half cycle of an oscillation). Red color indicates greater connectivity during successful encoding. Inset rose plot shows the mean phase difference for the selected time–frequency window (the blue oval) for an individual electrode pair, consistent with existing data and the example given in a. Phase difference of $+15^\circ$ indicates the ventral contacts are ahead of dorsal contacts, consistent with dorsal–ventral direction of propagation. (c) Shows the mean speed of propagation (histogram) for each subject. (d) Shows the results of a phase reset SME analysis, comparing phase dispersion during recalled and nonrecalled events. SME Z value (*t*-test across subjects comparing phase reset in recalled versus nonrecalled events) is plotted. The SME magnitude is not strong, but the difference in the timing of the maximum phase reset between the two locations is also consistent with dorsal–ventral propagation of a slow theta wave [Color figure can be viewed at wileyonlinelibrary.com]

anatomical origin of the signal. We compared PLS values during successful versus unsuccessful item encoding to identify time–frequency points for which there was a connectivity subsequent memory effect. For the 2.5–5 Hz slow theta oscillation, there was increased anterior–posterior connectivity centered at 1,000 ms after item presentation for nearly one full cycle of the oscillation, indicating there is greater connectivity at this frequency within the hippocampus during successful encoding ($p < .05$, paired *t*-test between recalled and nonrecalled PLS distributions, 222 electrode pairs). The average phase difference between these locations for successful encoding events ($\varphi_{\text{anterior}} - \varphi_{\text{posterior}}$) was $+9.2 \pm 12.3$ degrees. The observed phase offset may be consistent with existing data suggesting oscillations at this frequency are best modeled as a traveling wave propagating along the longitudinal axis of the hippocampus (Zhang & Jacobs, 2015). For each subject with anterior–posterior electrode pairs, we calculated a speed of propagation for such a putative traveling wave using the phase difference between the locations in this same frequency range (during the

coherent segments of the time series) and the distance between the contacts (average was 24 mm). The subject-level histogram for this calculation is shown in Figure 3, lower left. The mean speed for such a wave across subjects is 1.62 ± 0.23 m/s, consistent with values in the 3–5 Hz range previously reported in humans (Zhang & Jacobs, 2015).

To further characterize the properties of this oscillation, we examined phase reset in the anterior and posterior hippocampus. Phase reset involves quantifying the phase dispersion across events at each time sample following the onset of a study item; this is not a measure of connectivity as phase dispersion is quantified (using the Rayleigh test) *within* a brain location (in this case, separately for anterior and posterior electrodes). Results are shown in Figure 3, lower right panel. In the first half of the time series, there is greater reset of phase for successfully encoded items (Z value greater than zero) for both anterior and posterior hippocampal electrodes, but reset of phase occurs earlier in the time series in the posterior contacts. The timing of this phase reset

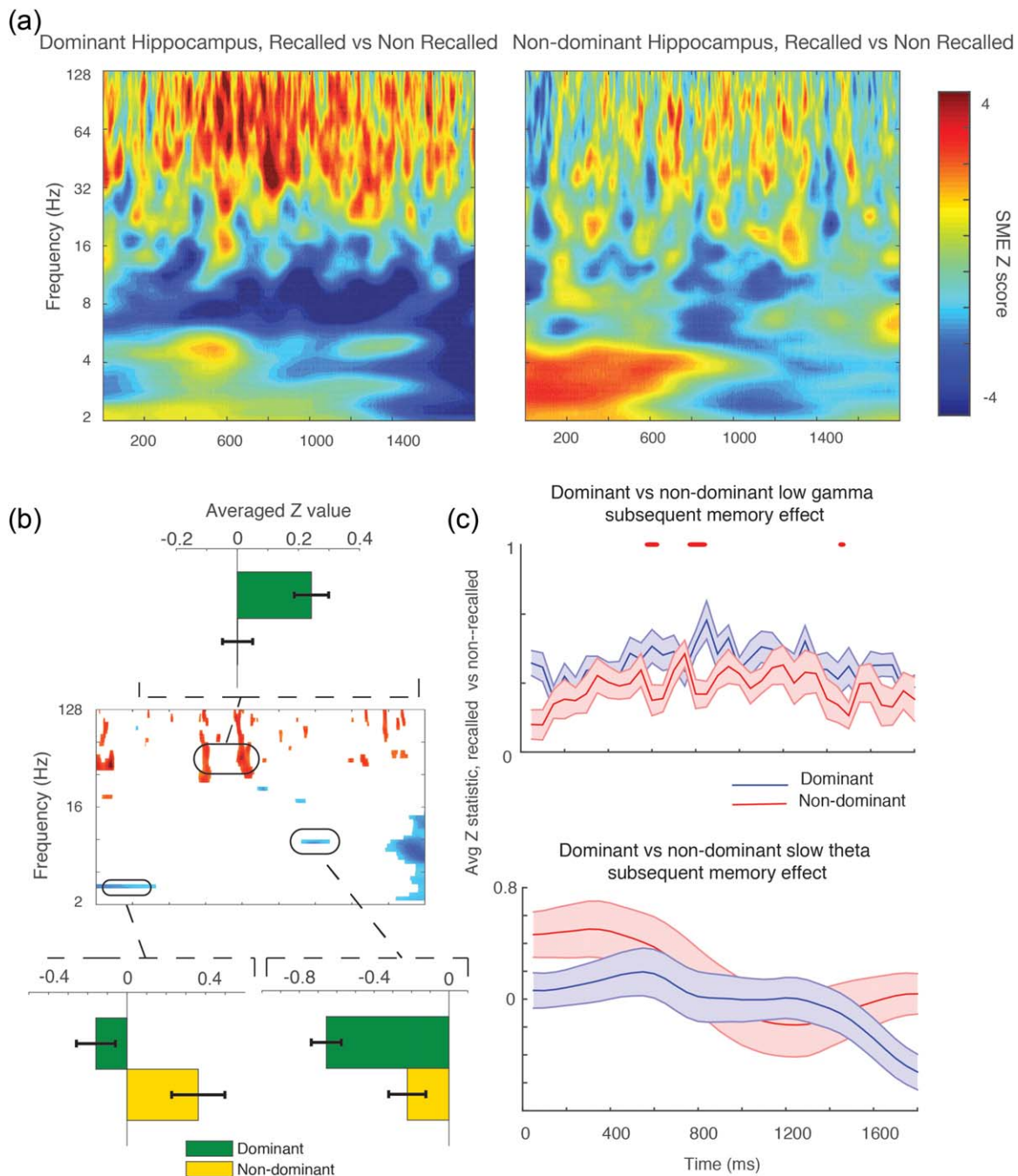


FIGURE 4 Dominant versus nondominant hemisphere SME. (a) Aggregate subsequent memory effect across all electrodes (effect size) in dominant (left panel) and nondominant (right panel) time–frequency plots. (b) Center shows time–frequency pixels across all subjects (t -test across 18 subjects contributing dominant and 17 subjects contributing nondominant electrodes) that meet requirement of $p < .05$ for one continuous half cycle of the oscillation. Inset bar plot above shows average gamma band SME Z value in the highlighted window, showing a larger effect in the dominant hemisphere. Lower inset plots show a large slow-theta effect for the nondominant hemisphere, although this does not survive Bonferroni's correction (shown in c). Negative SME observed at 9 Hz is stronger in the dominant hemisphere. (c) SME Z values between dominant and nondominant electrodes (averaged within subject) across the time series for the gamma band (top) and slow theta band (bottom). Red tick marks indicate time points at which SME difference survives Bonferroni's correction for one continuous half cycle of the oscillation. Although there is a difference at the beginning of the time series in the slow-theta range, it does not survive correction [Color figure can be viewed at wileyonlinelibrary.com]

SME is consistent with a model of a posterior–anterior traveling wave in that reset occurs earlier in the posterior hippocampus. However, these analyses cannot rule out the possibility that theta oscillations

with separate anterior and posterior (or some third location) generators respond to memory stimuli sequentially in time, a point we address directly in the “Section 4”.

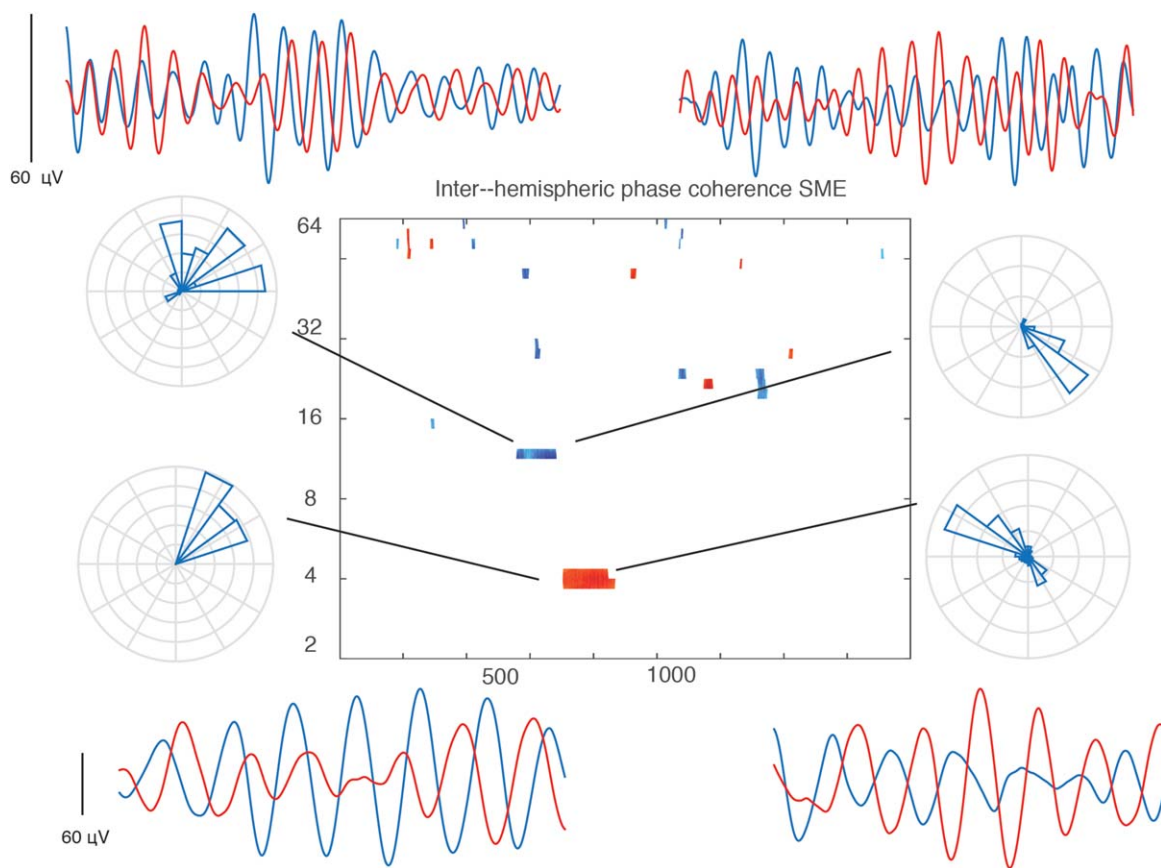


FIGURE 5 Interhippocampal connectivity during item encoding time–frequency plot at center shows pixels across 12 subjects (t -test between recalled and nonrecalled PLS distributions) that exhibit a significant SME ($p < .05$ for one continuous half cycle of oscillation), indicating greater connectivity during successful item encoding between left and right hippocampi at 4 Hz. There is decreased connectivity at ~ 10 Hz. Red colors indicate greater connectivity during successful encoding, blue colors indicate less connectivity. Surrounding plots are individual examples of filtered waves (single trials from individual electrodes, one from each hemisphere, 1800 ms time series) and rose plot histograms indicate there is significant heterogeneity in the phase offset across electrodes for each frequency range, precluding any inferences regarding left–right directionality from these data [Color figure can be viewed at wileyonlinelibrary.com]

3.2 | Hemispheric differences in subsequent memory effects

We compared the subsequent memory effect for dominant (76) and nondominant (65) electrodes by first quantifying a subsequent memory effect (recalled versus nonrecalled events, Z values from shuffle procedure) for electrodes from each hemisphere, and then contrasted these distributions directly using a t -test across subjects (analogs to the anterior–posterior comparison described above, $t(33) > 1.7$ for one half continuous oscillatory cycle). Results are shown in Figure 4. There is a significantly greater positive gamma band SME especially in the middle of the time series in the *dominant* hippocampus; this survives Bonferroni's correction for a continuous half cycle (Figure 4, right side) at several points ($p < .05$, corrected across 6 frequency bands). For the 2.5–5 Hz slow-theta oscillation by contrast, there is a positive SME in the first half of the time series in the nondominant hippocampal electrodes, although this effect does not survive Bonferroni's correction across subjects for a continuous half cycle of the oscillation.

We followed up on this analysis by examining dominant–nondominant phase synchrony during successful and unsuccessful memory

encoding; this analysis was restricted to subjects who had both left and right sided electrodes (12 subjects), which were exclusively in the ventral hippocampus based on clinical practice. We compared the distribution of PLS values for recalled versus nonrecalled events. The results are shown in Figure 5. A significant difference in PLS values between the distributions is found between 600 and 900 ms after item presentation for oscillations centered both at 4 and at 9–10 Hz. These effects go in opposite directions: the 4 Hz oscillation exhibited an increase in phase coherence (greater coupling) during successful encoding, while the 9 Hz oscillation exhibits a decrease. Phase coherence during recalled events for this window yielded an average phase difference of $+88^\circ \pm 20.3^\circ$ $\varphi_{\text{dominant}} - \varphi_{\text{nondominant}}$ for dominant and nondominant hippocampi, although there was significant heterogeneity among electrode pairs (ranging from 35° to 285°) for both oscillations. This is reflected in the examples from individual electrode pairs surrounding the central plot in Figure 5, and it implies that while many subjects exhibit differential connectivity during successful encoding between left and right hippocampi, the preferred phase of interhippocampal coupling is quite variable.

This finding, along with the more complex interhemispheric circuitry (as compared to the within-hippocampus analysis described above) makes it difficult to hypothesize if one hemisphere is “leading” the other using this analysis.

3.3 | Retrieval power analysis

We repeated the dominant–nondominant and anterior–posterior power comparisons for the retrieval phase of the free recall task. For this analysis, correct retrieval events (excluding list intrusions) were compared to randomly selected one second time epochs sampled from within the retrieval period that were temporally distant from a recall event (see Section 2). The average effects across anterior and posterior electrode contacts are illustrated in Figure 6, panel A. A broad low-frequency power decrease is visible along with a gamma band power increase that is most pronounced in the immediate 200 ms prior to vocalization of a retrieved memory item. Anterior–posterior differences that survive correction at the subject level are limited to rare time-points in the gamma and beta band; these do not survive correction. The same broad gamma band power increase is visible in the dominant and nondominant hippocampi, but it is of greater magnitude (greater gamma power increase before item vocalization) in the nondominant hemisphere, especially at the end of the time series. We tested for hemispheric differences in this gamma band retrieval effect using methods analogous to those described above (*t*-test at the subject level across the distributions of *Z* values). The difference survives Bonferroni’s correction for multiple cycles within the time series in the high-gamma range. The low frequency power decrease is stronger and more broad in the dominant hemisphere (Figure 6, panel B) but this difference is significant only for sporadic time points and it does not survive Bonferroni’s correction. Overall, the dominant–nondominant comparison is a reversal of the effect during item encoding, for which the gamma band subsequent memory effect is stronger in the dominant hemisphere. Since the retrieval effects were calculated relative to a baseline period, we wanted to make sure this apparently greater increase in gamma power in the nondominant hemisphere was not due to lower baseline gamma power during this period (artificially inflating the gamma effect we observed relative to the dominant hemisphere). We tested for this possibility by randomly selecting baseline power values, normalizing them and then comparing these directly (separately for low gamma and high gamma) between the dominant and nondominant hemispheres. Baseline gamma power in both bands was higher for nondominant hemisphere, consistent with an elevation of power in this frequency range that increases immediately before item vocalization but occurs throughout the retrieval period. It indicates that baseline differences do not account for the greater gamma power elevation in the nondominant hemisphere observed in the event-locked data shown in Figure 6. If anything, our method of comparing to a baseline condition might slightly understate the magnitude of the hemispheric differences in the 1000 ms preceding vocalization of a retrieved memory item.

4 | DISCUSSION

4.1 | Anterior–posterior differences in hippocampal function

Our examination of anterior versus posterior hippocampal oscillatory activity showed that while the gamma band subsequent memory effect is similar between both locations, there is a positive slow-theta SME exclusively in the posterior hippocampus. Explicating this anatomical difference in oscillatory activity provides human evidence of dorsal–ventral differences in hippocampal function observed in rodent data. Results in rodents include the observation that place cells in the dorsal hippocampus have more precise spatial fields than those found in the ventral hippocampus; this difference in place fields is preserved in non-human primates (Killiany et al., 2002; Strange et al., 2014). Classical horseradish peroxidase studies suggest a difference in the anatomical segregation of hippocampal efferent fibers between dorsal and ventral regions including preferential projection of the ventral hippocampus to the amygdala (Meibach & Siegel, 1977a, 1977b; Pitkänen, Pikkarainen, Nurminen, & Ylinen, 2000; Strange et al., 2014), and whole exome sequencing has identified sharp demarcations in gene expression pattern along the hippocampal axis. These structural and functional differences, preserved across species, motivated our hypothesis that we would observe differences in anterior versus posterior slow theta and gamma activity during memory encoding.

One might reasonably ask if the dorsal–ventral differences in the rodent hippocampus can be expected to apply to humans; in humans the ventral region (adjacent to the amygdala) has undergone relatively greater expansion compared to the dorsal portions of the hippocampus [for a review, see Box 1 in Strange et al. (2014)]. Functional imaging and lesion data has suggested the posterior hippocampus in humans shows preferential activity during spatial navigation in the nondominant hemisphere (Abrahams et al., 1997; Pu et al., 2017), although this has not reliably been demonstrated for verbal memory tasks in the dominant hemisphere or with intracranial EEG, in which aggregated hippocampal electrodes have been shown to exhibit theta power decreases and gamma band power increases during memory encoding (Sederberg et al., 2007). However, to our knowledge, there has not been a systematic attempt to differentiate anterior and posterior hippocampal electrodes and directly compare oscillatory effects. Generally, our data support the hypothesis that memory encoding-related neural activity in the human hippocampus differs along the longitudinal axis, in that we observed a robust difference in the modulation of slow-theta oscillatory activity between the anterior and posterior hippocampus. However, we did not observe an anterior–posterior difference in the gamma band positive subsequent memory effect or the ~9 Hz negative SME that have been previously described for the hippocampus (Sederberg et al., 2007).

Several models of differential hippocampal function along the ventral–dorsal (anterior–posterior in primates) have been proposed. A model proposed by Moser and Moser (1998) and elaborated by Fanselow and Dong (2010) proposes that the ventral region exhibits sensitivity to emotional content of successfully retrieved memory items, while

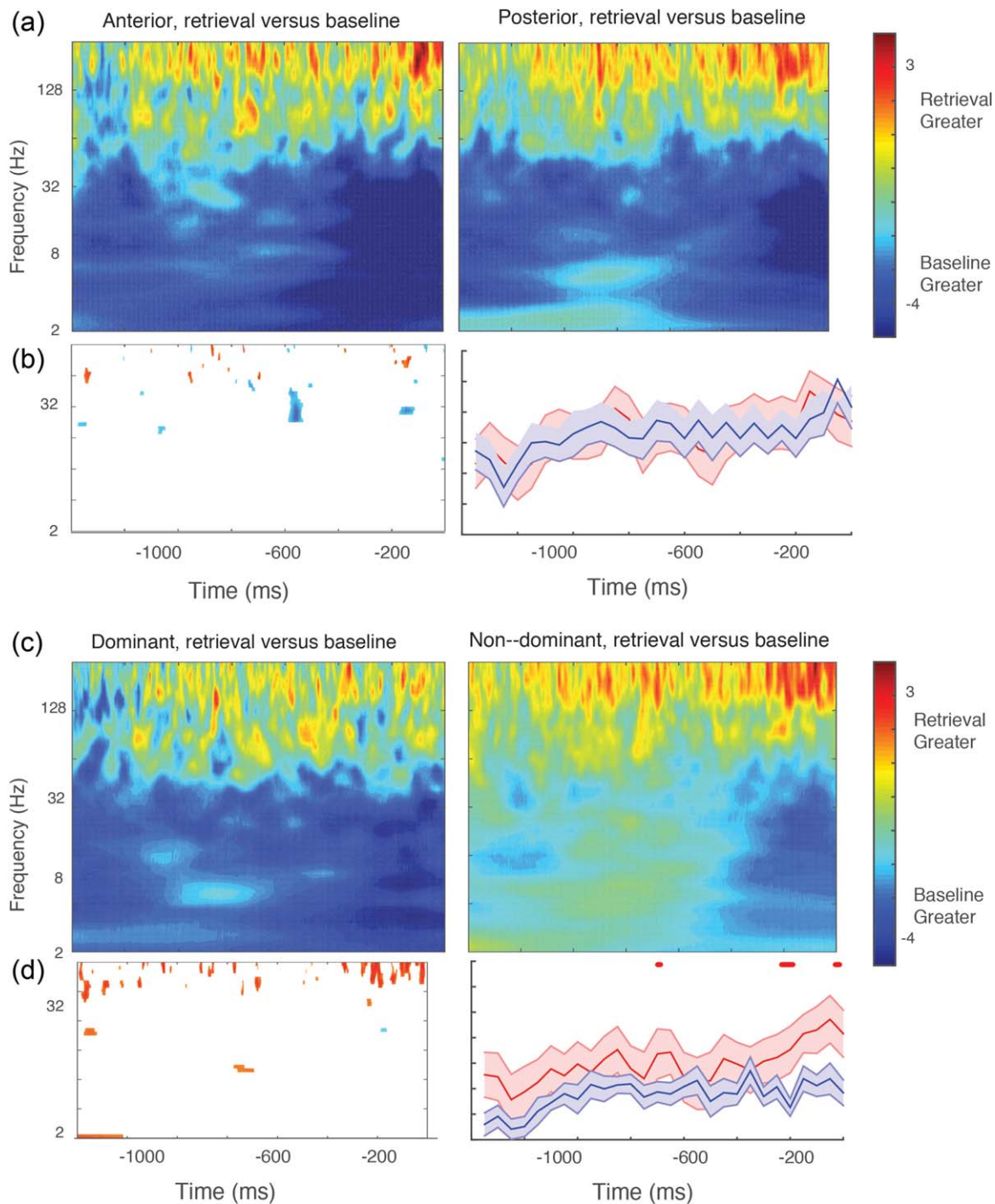


FIGURE 6 Oscillatory power during item retrieval. (a) The results of t-test comparing retrieval effect size across all electrodes between anterior and posterior electrode groups. (b) Time–frequency points across all electrodes that exceed $p < .05$ for one continuous cycle of an oscillation; this is limited brief differences between anterior and posterior hippocampi in the beta frequency range, related to a greater power decrease relative to baseline in the posterior electrodes. Right in B shows results for gamma frequency range across 23 subjects; no points survive Bonferroni's correction for one continuous half cycle. (c) The comparison between the dominant and nondominant hemisphere across all electrodes. The low frequency power decrease occurs immediately prior to item retrieval in the nondominant hemisphere versus throughout the time series in the dominant hemisphere, visible in the direct comparison between electrode sets in d, left plot. The most striking difference is in the high gamma range, for which a power increase relative to baseline is stronger in the nondominant hemisphere. This difference survives Bonferroni's correction at the subject level (d, right) [Color figure can be viewed at wileyonlinelibrary.com]

the dorsal hippocampus is implicated preferentially in encoding the nonemotional content or context for an individual item. Our results do not directly address this proposal, insofar as the affective content of the memory items was not manipulated, although our observation that the anterior hippocampus exhibits a robust gamma range SME on par with the posterior hippocampus suggests that both regions are involved in representing features of the memory items. Without manipulating affective content directly, it is not possible to discern whether the anterior gamma SME is related exclusively to such a feature of the memory items, while posterior gamma is related to nonaffective features of the items. Fanselow and Dong (2010) also discuss a more general theory of hippocampal specialization, by which the anterior hippocampus supports pattern completion while the posterior hippocampus performs pattern separation. A related view articulated by Poppenk et al. (2013) posits that there is a change in the “gain of representation” along the dorsal–ventral axis, with more general information represented in anterior hippocampus and more specific contextual information represented in the posterior hippocampus. This theory is most easily understood in terms of spatial navigation, as the anterior hippocampus would represent more general location information while the posterior hippocampus would represent precise information of a specific location. The authors propose that, for episodic memory, this would entail greater representation of contextual details in the posterior hippocampus, although human fMRI data have not observed stronger posterior activation (Rugg & Vilberg, 2013). This theory can account for many animal observations including place field specificity and connectivity-related differences along the hippocampal axis. Without a definitive assessment of the relative contribution of slow-theta versus gamma oscillations in supporting episodic memory, it is difficult to argue if our data directly support this view. A memory task that manipulates the specificity of memories during retrieval, perhaps incorporating both item and category information, may help address this question.

4.2 | Slow-theta oscillations in humans and rodents

Our data add to the growing literature examining subtleties in low frequency activity in the human mesial temporal lobe during the encoding of episodic memories. Previous work has suggested that there is a broad decrease in power in the hippocampus during successful memory encoding, but that a select subpopulation of electrodes exhibits power increases in a band spanning the traditional delta-theta range, from 2.5 to 5 Hz (Lega, Jacobs, & Kahana, 2011). The results we present here suggest that when SME data is aggregated across many anterior and posterior hippocampal contacts (and the time series is collapsed after item presentation) the overall pattern is a *negative* SME across the entire 2–11 Hz frequency range (Lega et al., 2011; Sederberg et al., 2007), but that segregating electrodes according to position along the long axis and preserving the time series information reveals a positive effect in the posterior contacts in the slow-theta range. Connectivity data has suggested brain regions are coupled via activity in this frequency range immediately prior to memory items that are successfully encoded (Haque, Wittig, Damera, Inati, & Zaghoul, 2015), and

also that parietal–hippocampal interaction at this frequency range (though also at other frequencies) is increased during successful item retrieval (Watrous et al., 2013). The evidence for slow-theta power increases during mnemonic processing has been mixed, however: a recent noninvasive study using iEEG and MEG failed to show power increases in the hippocampus during spatial navigation (Crespo-García et al., 2016) for example. The data we present here is drawn from patients undergoing stereo EEG; this technique is better-suited to investigating anterior–posterior differences in hippocampal oscillatory activity because it permits precise targeting separately to the head and tail of the hippocampus. Depth electrodes with contacts along the hippocampal axis have previously revealed evidence of activity in the 2.5–5 Hz range in both the anterior and posterior region, though this has not been linked to differences in memory encoding (Zhang & Jacobs, 2015), while a study with similar methods identified differences in adjacent-pair signal coherence in the ventral–dorsal transition (Staresina, Henson, Kriegeskorte, & Alink, 2012).

Evidence for a theta gradient along the dorsal–ventral axis in the rodent literature links greater spike-field coherence for CA3 cells in the dorsal hippocampus to greater place cell specificity [for a summary of rodent results, see Section 4 in Royer, Sirota, Patel, and Buzsáki, 2010]. Royer et al. (2010) also identified relatively less power for theta oscillations in the ventral versus dorsal hippocampus during spatial navigation, though as with our study there was strong coherence in these oscillations between dorsal and ventral locations. The authors hypothesized that the paucity of human evidence for strong theta activity may reflect the expansion of the ventral hippocampus relative to dorsal sections in primate evolution (diminishing the theta source). We would add that the pattern of electrode implantation typically employed in seizure localization efforts likely also contributes to this disparity between the human and animal literature.

Data comparing activity in human CA1 versus CA3 may be relevant to our results: in humans, CA1 is relatively expanded in the anterior hippocampus, and fMRI experiments suggest greater CA3 activation for pattern separation (identifying lures) versus pattern completion (hits) when CA1 activity is greater (Bakker, Brock Kirwan, Miller, & Stark, 2008). These data however did not suggest a significant difference in BOLD activation along the longitudinal axis. If CA3 is more directly responsible for generating the slow theta positive SME as suggested by rodent data (Buzsáki, 2002), its relatively greater representation (relative to the size of CA1) in the posterior hippocampus might explain our results. We made a preliminary attempt at resolving differences in slow-theta activity among hippocampal subfields that is presented in the Supporting Information Material section, but our data set is not well-suited to this question. Resolving the issue of the contribution of different hippocampal subfields to the slow-theta SME will likely require microelectrode recordings with more precise intrahippocampal targeting. Ideally, comparisons of anterior–posterior slow-theta activity would be performed within the same subfield. Our dataset also suffers a related limitation, namely an inability to resolve differences among the *three* hippocampal sectors (anterior, middle, and posterior) rather than two (anterior vs. posterior) (Strange et al., 2014).

4.3 | Traveling wave properties of human hippocampal slow theta oscillations

A previous study directly examined theta oscillations along the longitudinal axis in the human hippocampus using occipital depth electrodes; its results were thought to be most consistent with theta oscillations acting as traveling waves along this axis (Zhang & Jacobs, 2015). The reported propagation speed (approximately 1.2–2 m/s) and magnitude of the phase change along the hippocampal axis matches what we calculated using our own data. The estimated speed of propagation of rodent hippocampal oscillations for the predominant 8 Hz oscillation is 0.16 m/s, although this seemed to vary with behavior (Patel, Fujisawa, Berényi, Royer, & Buzsáki, 2012). It is important to note that in our data, the phase coherence between dorsal and ventral hippocampus was significantly stronger during the encoding of later recalled than later forgotten study items, which raises the possibility that coherent traveling theta waves arise in the hippocampus preferentially during periods of successful episodic encoding. This observation suggests that intrahippocampal integration in these lower frequency ranges supports mnemonic processing.

There are of course competing explanations for our observations. The consistent phase offset between dorsal and ventral hippocampal locations could be due to a common theta generator propagating to both locations; our dataset is not capable of resolving this question which requires recordings from electrode contacts placed continuously along the anterior–posterior axis. But a model of multiple theta “repeaters” along the dorsal–ventral axis with a theta source in the septum fits well with the phase reset data we present (Lubenov & Siapas, 2009), and the relatively narrow phase difference between locations is more likely due to a traveling wave than two independent theta oscillations (one in each location) that exhibit phase coherence. A lower phase shift per unit distance for the relevant theta frequency in the human hippocampus as compared to rodents would theoretically permit greater integration of activity along the longitudinal axis (Zhang & Jacobs, 2015), especially if the phase difference along the full axis is less than a half cycle of the oscillation (facilitating simultaneous potentiation of membrane effects). In rodents, variability of the speed of propagation has also been observed for a hippocampal traveling wave (Lubenov & Siapas, 2009), similar to our results illustrated in the histogram in Figure 3.

4.4 | Hemispheric differences in hippocampal oscillatory properties

There is an extensive literature describing the memory deficits associated with seizure onset or lesions in either dominant or nondominant hemisphere (Bonelli et al., 2010; Abrahams et al., 1997; Pu et al., 2017). Commensurate with these clinical observations, right lateralized hippocampal oscillations have been observed in humans in spatial memory tasks (Cornwell, Johnson, Holroyd, Carver, & Grillon, 2008; Ekstrom et al., 2005; Jacobs et al., 2010). However, a matching difference in the gamma band SME for episodic memory processing has not been observed in previous studies (Sederberg et al., 2007). Our data

demonstrate a stronger gamma band positive SME in the dominant hemisphere (during encoding). Insofar as the hippocampus represents or indexes cortical representations of individual memory items, this left-lateralized signal may be an oscillatory correlate of the representation of semantic features of the study words (Evans & Federmeier, 2007). The left–right difference in the 9 Hz power decrease matched the gamma band effect. Left–right connectivity has not been extensively studied in human intracranial EEG, owing to the relative rarity of strong bihemispheric sampling from subjects performing episodic memory tasks. Our results implicate a transient elevation in connectivity during successful encoding in the slow-theta range. Interhippocampal functional connectivity has been linked to memory performance in young adults (Wang et al., 2010) and victims of traumatic brain injury (de la Plata et al., 2011). This connectivity may reflect the integrity of the dorsal hippocampal commissure (Gloor, Salanova, Olivier, & Quesney, 1993), although other pathways including the uncinate fasciculus may also contribute (Diehl et al., 2008).

During successful recall, we observed a gamma band power increase that preceded vocalization of the retrieved memory item; this effect was stronger in the *nondominant* hemisphere, in opposition to the pattern we observed during encoding. This finding is hard to reconcile with the previously reported recapitulation of encoding-related oscillatory patterns during item retrieval (Manning, Polyn, Baltuch, Litt, & Kahana, 2011), although this may reflect a failure to distinguish between hemispheres when quantifying hippocampal activity at retrieval. It is interesting that the present hemispheric difference occurs in the high gamma range principally, while the asymmetry in the encoding gamma related effect occurs across the entire gamma spectrum. It will be informative to observe how electrical stimulation of one hippocampus alters oscillatory patterns in the other during mnemonic processing, and how more subtle item-context manipulations affect the hemispheric gamma band differences in gamma band power changes during retrieval. We note in passing that the present findings that encoding-related gamma effects were left lateralized, while retrieval-related effects were more prominent on the right, are reminiscent of the ‘HERA’ principle held at one time to apply to the prefrontal cortex (Babiloni et al., 2006; Habib, Nyberg, and Tulving, 2003). While we are unaware of any prior evidence suggesting that this principle applies to the hippocampus, it is possible that our findings are indicative of a division of labor along these lines.

5 | CONCLUSION

Using electrodes precisely targeted to the anterior and posterior hippocampus, we observed a difference in an SME in the slow-theta (3.5–5 Hz) frequency range indicating that the posterior but not anterior hippocampus exhibits a power increase during successful item encoding. Connectivity analyses suggested that intrahippocampal phase coherence at this frequency also predicts successful item encoding, and that oscillations at this frequency propagate along the longitudinal axis possibly as a traveling wave. Differences in slow-theta activity during encoding along the axis of the hippocampus may be consistent

with postulated differences in the functional specialization of the anterior versus posterior hippocampus, including more detailed representation of temporal or spatial context information in the posterior hippocampus. While the gamma band positive SME was not significantly different in anterior and posterior hippocampi, we did observe differences in the SME at this frequency band between the dominant and nondominant hemispheres. This hemispheric asymmetry may reflect greater activity related to the representation of the semantic content of encoded memory items in the dominant hemisphere, although the reversal of this pattern during item retrieval makes this result more difficult to interpret.

ACKNOWLEDGMENTS

Funding in part via UT Brain Seed Grant #366582, NIH R21 NS095094 and DARPA Restoring Active Memory project. We thank Blackrock Microsystems for providing neural recording and stimulation equipment. This work was supported by the DARPA Restoring Active Memory (RAM) program (Cooperative Agreement N66001-14-2-4032). The views, opinions, and/or findings contained in this material are those of the authors and should not be interpreted as representing the official views or policies of the Department of Defense or the U.S. Government.

CONFLICT OF INTEREST

The authors declare no competing conflicts of interest.

REFERENCES

- Abrahams, S., Pickering, A., Polkey, C. E., & Morris, R. G. (1997). Spatial memory deficits in patients with unilateral damage to the right hippocampal formation. *Neuropsychologia*, 35(1), 11–24.
- Babiloni, C., Vecchio, F., Cappa, S., Pasqualetti, P., Rossi, S., Miniussi, C., & Maria Rossini, P. (2006). Functional frontoparietal connectivity during encoding and retrieval processes follows her model: A high-resolution study. *Brain Research Bulletin*, 68(4), 203–212.
- Bakker, A., Brock Kirwan, C., Miller, M., & Stark, C. E. L. (2008). Pattern separation in the human hippocampal ca3 and dentate gyrus. *Science*, 319(5870), 1640–1642.
- Bohbot, V. D., Kalina, M., Stepankova, K., Spackova, N., Petrides, M., & Nadel, L. Y. N. (1998). Spatial memory deficits in patients with lesions to the right hippocampus and to the right parahippocampal cortex. *Neuropsychologia*, 36(11), 1217–1238.
- Bonelli, S. B., Powell, R. H., Yogarajah, W. M., Samson, R. S., Symms, M. R., Thompson, P. J., ... Duncan, J. S. (2010). Imaging memory in temporal lobe epilepsy: Predicting the effects of temporal lobe resection. *Brain*, awq006.
- Burke, J. F., Sharan, A. D., Sperling, M. R., Ramayya, A. G., Evans, J. J., Healey, M. K., ... Kahana, M. J. (2014). Theta and high-frequency activity mark spontaneous recall of episodic memories. *The Journal of Neuroscience*, 34(34), 11355–11365.
- Buzsáki, G. (2002). Theta oscillations in the hippocampus. *Neuron*, 33(3), 325–340.
- Cornwell, B. R., Johnson, L. L., Holroyd, T., Carver, F. W., & Grillon, C. (2008). Human hippocampal and parahippocampal theta during goal-directed spatial navigation predicts performance on a virtual Morris water maze. *Journal of Neuroscience*, 28(23), 5983–5990.
- Crespo-García, M., Zeiller, M., Leupold, C., Kreiselmeier, G., Rampp, S., Hamer, H. M., & Dalal, S. S. (2016). Slow-theta power decreases during item-place encoding predict spatial accuracy of subsequent context recall. *NeuroImage*, 142, 533–543.
- de la Plata, C. D. M., J., Garces, E., Shokri Kojori, J., Grinnan, K., Krishnan, R., Pidikiti, J., ... Diaz-Arrastia, R. (2011). Deficits in functional connectivity of hippocampal and frontal lobe circuits after traumatic axonal injury. *Archives of Neurology*, 68(1), 74–84.
- Diehl, B., Busch, R. M., Duncan, J. S., Piao, Z., Tkach, J., & Lüders, H. O. (2008). Abnormalities in diffusion tensor imaging of the uncinate fasciculus relate to reduced memory in temporal lobe epilepsy. *Epilepsia*, 49(8), 1409–1418.
- Ekstrom, A. D., Caplan, J. B., Ho, E., Shattuck, K., Fried, I., & Kahana, M. J. (2005). Human hippocampal theta activity during virtual navigation. *Hippocampus*, 15, 881–889.
- Ekstrom, A., Nanthia, S., David, M., Itzhak, F., & Susan, B. (2009). Correlation between bold fmri and theta-band local field potentials in the human hippocampal area. *Journal of Neurophysiology*, 101(5), 2668–2678.
- Evans, K. M., & Federmeier, K. D. (2007). The memory that's right and the memory that's left: Event-related potentials reveal hemispheric asymmetries in the encoding and retention of verbal information. *Neuropsychologia*, 45(8), 1777–1790.
- Ezzati, A., Katz, M. J., Zammit, A. R., Lipton, M. L., Zimmerman, M. E., Sliwinski, M. J., & Lipton, R. B. (2016). Differential association of left and right hippocampal volumes with verbal episodic and spatial memory in older adults. *Neuropsychologia*, 93, 380–385.
- Fanselow, M. S., & Dong, H.-W. (2010). Are the dorsal and ventral hippocampus functionally distinct structures? *Neuron*, 65(1), 7–19.
- Fletcher, P. C., Frith, C. D., & Rugg, M. D. (1997). The functional neuroanatomy of episodic memory. *Trends in Neurosciences*, 20(5), 213–218.
- Gloor, P., Salanova, Olivier, V. A., & Quesney, L. F. (1993). The human dorsal hippocampal commissure. *Brain*, 116(5), 1249–1273.
- Gonzalez-Martinez, J., Bulacio, J., Alexopoulos, A., Jehi, L., Bingaman, W., & Najm, I. (2013). Stereoelectroencephalography in the "difficult to localize" refractory focal epilepsy: Early experience from a North American epilepsy center. *Epilepsia*, 54(2), 323–330.
- Greicius, M. D., Krasnow, B., Boyett-Anderson, J. M., Eliez, S., Schlaggar, A. F., Reiss, A. L., & Menon, V. (2003). Regional analysis of hippocampal activation during memory encoding and retrieval: FMRI study. *Hippocampus*, 13(1), 164–174.
- Habib, R., Nyberg, L., & Tulving, E. (2003). Hemispheric asymmetries of memory: The Hera model revisited. *Trends in Cognitive Sciences*, 7(6), 241–245.
- Haque, R. U., Wittig, J. H., Damara, S. R., Inati, S. K., & Zaghoul, K. A. (2015). Cortical low-frequency power and progressive phase synchrony precede successful memory encoding. *The Journal of Neuroscience*, 35(40), 13577–13586.
- Henke, P. G. (1990). Granule cell potentials in the dentate gyrus of the hippocampus: Coping behavior and stress ulcers in rats. *Behavioural Brain Research*, 36(1–2), 97–103.
- Jacobs, J., Korolev, I. O., Caplan, J. B., Ekstrom, A. D., Litt, B., Baltuch, G., ... Kahana, M. J. (2010). Right-lateralized brain oscillations in human spatial navigation. *Journal of Cognitive Neuroscience*, 22(5), 824–836.
- Jacobs, J. (2014). Hippocampal theta oscillations are slower in humans than in rodents: Implications for models of spatial navigation and memory. *Philosophical Transactions of the Royal Society of London B: Biological Sciences*, 369(1635), 20130304.

- Killiany, R. J., Hyman, B. T., Gomez-Isla, T., Moss, M. B., Kikinis, R., Jolesz, F., ... Albert, M. S. (2002). MRI measures of entorhinal cortex vs hippocampus in preclinical ad. *Neurology*, 58(8), 1188–1196.
- Lachaux, J. P., Rodriguez, E., Martinerie, J., & Varela, F. J. (1999). Measuring phase synchrony in brain signals. *Human Brain Mapping*, 8(4), 194–208.
- Lega, B. C., Jacobs, J., & Kahana, M. J. (2011). Human hippocampal theta oscillations and the formation of episodic memories. *Hippocampus*, 22(4), 748–761.
- Lubenov, E. V., & Siapas, A. G. (2009). Hippocampal theta oscillations are travelling waves. *Nature*, 459(7246), 534–539.
- Maggio, N., & Segal, M. (2009). Differential modulation of long-term depression by acute stress in the rat dorsal and ventral hippocampus. *The Journal of Neuroscience*, 29(27), 8633–8638.
- Manning, J. R., Polyn, S. M., Baltuch, G., Litt, B., & Kahana, M. J. (2011). Oscillatory patterns in temporal lobe reveal context reinstatement during memory search. *Proceedings of the National Academy of Sciences USA*, 108(31), 12893–12897.
- Matus-Amat, P., Higgins, E. A., Barrientos, R. M., & Rudy, J. W. (2004). The role of the dorsal hippocampus in the acquisition and retrieval of context memory representations. *The Journal of Neuroscience*, 24(10), 2431–2439.
- Meibach, R. C., & Siegel, A. (1977a). Efferent connections of the hippocampal formation in the rat. *Brain Research*, 124(2), 197–224.
- Meibach, R. C., & Siegel, A. (1977b). Efferent connections of the septal area in the rat: an analysis utilizing retrograde and anterograde transport methods. *Brain Research*, 119(1), 1–20.
- Moser, E. I., Moser, M. B., & Andersen, P. (1993). Spatial learning impairment parallels the magnitude of dorsal hippocampal lesions, but is hardly present following ventral lesions. *Journal of Neuroscience*, 13(9), 3916.
- Moser, M. B., & Moser, E. I. (1998). Functional differentiation in the hippocampus. *Hippocampus*, 8(6), 608–619.
- Patel, J., Fujisawa, S., Berényi, A., Royer, S., & Buzsáki, G. (2012). Traveling theta waves along the entire septotemporal axis of the hippocampus. *Neuron*, 75(3), 410–417.
- Pitkänen, A., Pikkariainen, M., Nurminen, N., & Ylinen, A. (2000). Reciprocal connections between the amygdala and the hippocampal formation, perirhinal cortex, and postrhinal cortex in rat: A review. *Annals of the New York Academy of Sciences*, 911(1), 369–391.
- Poppenk, J., Evensmoen, H. R., Moscovitch, M., & Nadel, L. (2013). Long-axis specialization of the human hippocampus. *Trends in Cognitive Sciences*, 17(5), 230–240.
- Pu, Y., Cornwell, B. R., Cheyne, D., & Johnson, B. W. (2017). The functional role of human right hippocampal/parahippocampal theta rhythm in environmental encoding during virtual spatial navigation. *Human Brain Mapping*, 38(3), 1347–1361.
- Rizzuto, D. S., Madsen, J. R., Bromfield, E. B., Schulze-Bonhage, A., & Kahana, M. J. (2006). Human neocortical oscillations exhibit theta phase differences between encoding and retrieval. *NeuroImage*, 31(3), 1352–1358.
- Royer, S., Sirota, A., Patel, J., & Buzsáki, G. (2010). Distinct representations and theta dynamics in dorsal and ventral hippocampus. *The Journal of Neuroscience*, 30(5), 1777–1787.
- Rugg, M. D., & Vilberg, K. L. (2013). Brain networks underlying episodic memory retrieval. *Current Opinion in Neurobiology*, 23(2), 255–260.
- Ryan, L., Lin, C.-Y., Ketcham, K., & Nadel, L. (2010). The role of medial temporal lobe in retrieving spatial and nonspatial relations from episodic and semantic memory. *Hippocampus*, 20(1), 11–18.
- Sederberg, P. B., Schulze-Bonhage, A., Madsen, J. R., Bromfield, E. B., McCarthy, D. C., Brandt, A., ... Kahana, M. J. (2007). Hippocampal and neocortical gamma oscillations predict memory formation in humans. *Cerebral Cortex*, 17(5), 1190–1196.
- Sederberg, P. B., Kahana, M. J., Howard, M. W., Donner, E. J., & Madsen, J. R. (2003). Theta and gamma oscillations during encoding predict subsequent recall. *The Journal of Neuroscience*, 23(34), 10809–10814.
- Staresina, B. P., Henson, R. N. A., Kriegeskorte, N., & Alink, A. (2012). Episodic reinstatement in the medial temporal lobe. *The Journal of Neuroscience*, 32(50), 18150–18156.
- Strange, B. A., Witter, M. P., Lein, E. S., & Moser, E. I. (2014). Functional organization of the hippocampal longitudinal axis. *Nature Reviews Neuroscience*, 15(10), 655–669.
- Tallon-Baudry, C., Olivier, B., Claude, D., & Jacques, P. (1997). Oscillatory γ -band (30–70 Hz) activity induced by a visual search task in humans. *The Journal of Neuroscience*, 17(2), 722–734.
- Wang, L., Negreira, A., LaViolette, P., Bakkour, A., Sperling, R. A., & Dickerson, B. C. (2010). Intrinsic interhemispheric hippocampal functional connectivity predicts individual differences in memory performance ability. *Hippocampus*, 20(3), 345–351.
- Watrous, A. J., Fried, I., & Ekstrom, A. D. (2011). Behavioral correlates of human hippocampal delta and theta oscillations during navigation. *Journal of Neurophysiology*, 105(4), 1747–1755.
- Watrous, A. J., Lee, D. J., Izadi, A., Gurkoff, G. G., Shahlaie, K., & Ekstrom, A. D. (2013). A comparative study of human and rat hippocampal low-frequency oscillations during spatial navigation. *Hippocampus*, 23(8), 656–661.
- Zhang, H., & Jacobs, J. (2015). Traveling theta waves in the human hippocampus. *The Journal of Neuroscience*, 35(36), 12477–12487.

SUPPORTING INFORMATION

Additional Supporting Information may be found in the online version of this article.

How to cite this article: Lin J, Rugg M, Das S, et al. Theta band power increases in the posterior hippocampus predict successful episodic memory encoding in humans. *Hippocampus*. 2017; 27:1040–1053. <https://doi.org/10.1002/hipo.22751>